Thai Geoscience Journal 6(10), 2025, p. 26-50
Copyright © 2025 by the Department of Mineral Resources of Thailand
ISSN-2730-2695 (Print); ISSN-3056-9370 (Online); DOI-10.14456/tgj.2025.4

Permian radiolarian cherts and their geochemical characteristics in the Central Plain of Thailand: Implications for the geological affiliation and origin of the Permian chert.

Waraphorn Phromsuwan[1] Yoshihito Kamata[2] Thasinee Charoentitirat[3]
Katsumi Ueno[4] and Apsorn Sardsud[5]

[1]*Graduate School of Science and Technology, Degree Programs in Life and Earth Sciences, Doctoral Program in Geosciences, University of Tsukuba, Ibaraki, 305-8572, Japan*

[2] *Institute of Life and Environmental Sciences, Department of Geosciences, The University of Tsukuba, Tsukuba, Ibaraki, 305-8572, Japan*

[3] *Department of Geology, Faculty of Science, Chulalongkorn University, Bangkok 10330, Thailand*

[4] *Department of Earth System Science, Fukuoka University, Fukuoka 814-0180, Japan*

[5] *Department of Mineral Resources, Bangkok 10400, Thailand*

**Corresponding author*: *p.waraphorn245@gmail.com, yoshi_kamata@geol.tsukuba.ac.jp*

Received 27 May 2025; Revised 15 September 2025; Accepted 15 September 2025.

Abstract

Improved geological constraints refine our understanding of Southeast Asia's and Thailand's geotectonic evolution. This study investigates Permian chert successions in the Central Thailand, where are the Sawan Khalok and the Nakhon Sawan–Uthai Thani areas, to elucidate their genesis, depositional environment, and implications for the tectonic evolution. The Central Thailand is interpreted as part of the Sukhothai Zone characterized by an island arc setting such Permian-Triassic volcanic rocks, formed by the subduction of the Paleo-Tethys Ocean with the Indochina Block. Permian cherts, previously considered enigmatic, are irregularly distributed in this zone. The research examines four chert sections, identifying the Early Permian radiolarians (Asselian) in TS13, specifically *Pseudoalbaillella simplex* and *Pseudo-albaillella* cf. *annulata*, and late Early – early Middle Permian (Kungurian–Roadian) in TS14, comprising *Albaillella sinuata* and *Albaillella* cf. *asymmetrica*. The Middle Permian radiolarians (Roadian–Capitanian) identified include *Pseudoalbaillella scalprata*, *Parafollicucullus fusiformis*, *Parafollicucullinoides* cf. *globosus*, *Parafollicucullus monacanthus*, *Follicucullus* cf. *scholasticus*, and *Follicucullus* cf. *bipartitus* form NS07. For NS11, the identified radiolarians are *Pseudoalbaillella* cf. *lomentaria*, *Pseudoalbaillella scalprata, Parafollicucullus monacanthus*, and *Follicucullus* cf. *scholasticus* indicating Wordian–Capitanian ages.

Geochemical analyses (ICP-OES and ICP-MS) of chert samples from the four sections provide insights into their origin and depositional setting. Samples of TS13 and TS14 exhibit origins of hydrothermal influence and show a negative Ce anomaly, suggesting depositing nearby a spreading ridge environment with limited hydrothermal activity. Samples of NS07 and NS11 plot close to biogenic chert origin and display a depleted Ce anomaly, indicating decreased hydrothermal material input or deposition near a continental margin. Based on lithological characteristics and radiolarian ages, chert successions in the Sawan Khalok and the Nakhon Sawan–Uthai Thani areas are considered to have same origins of the Khanu Chert and the Khao Gob Chert. In terms of depositional time intervals and geochemistry characteristics, those of the cherts can correlate with cherts from the Sa Kaeo area, representing the Early and Middle Permian chert sequences, originated in a back-arc basin setting rather than formed in a vast oceanic

setting of the Paleo-Tethys Ocean. This study confirms an existence evidence of a back-arc basin chert in the Central Thailand, extending the known distribution of the Sa Kaeo suture zone northwestward from the Uthai Thani and Nakhon Sawan areas into the Sawan Khalok area, and continues toward the Nan suture. These stratigraphic relationships can be explained by the fact that the bedded cherts were thrust onto the structurally higher rocks of the Sukhothai Zone, due to lateral shortening tectonics associated with the closure of the back-arc basin.

Keywords: Back-arc basin, Central Thailand, Geochemistry, Permian, Radiolarian chert

1. Introduction

Thailand included Southeast Asia, which comprises numerous continental blocks that rifted from Gondwanaland during the early Paleozoic and integrated with each continental block during the mid-Mesozoic. Numerous researches have presented interpretations of the geotectonic development of Thailand and its surrounding areas (e.g., Hara et al., 2020, Metcalfe, 2013, 2021 and Ueno et al., 2018). According to their disclosures, the formation of a back-arc basin in the Paleo-Tethys region was a response to Paleo-Tethys subduction, which took place beneath the Sukhothai Volcanic Arc and the Indochina Block (Metcalfe, 2013, 2021). This basin is identified as sutures prolonging from southeastern to northeastern Thailand, including the Sa Kaeo and Nan suture zones **(Fig. 1)**. Prior studies indicate that these suture lines emerged from igneous rocks overlapped by specific rock assemblages, such Permian and Middle Triassic radiolarian chert, Permian limestone, and Triassic clastic sedimentary rock (Hada et al., 1999, Ito et al., 2020, Kamata et al., 2003, 2018, Saesaengseerung et al., 2009, Sashida et al., 1997, Udchachon et al., 2018). The original stratigraphy documents geological development of the back-arc basin from the Early Permian to the Late Triassic, reflecting its periods of opening and closure (Hara et al., 2018, Phromsuwan et al., 2024). Several studies of Permian sedimentary rocks, especially chert, fine-grained siliciclastic, and limestone, were discovered from the Central Plain of Thailand that it examined the depositional age of rock, conducted comprehensive investigations on microfossils, and analyzed tectonic implications in the Central Plain region (e.g., Fontaine et al., 1996, Saesaeng-seerung, 2009, Sashida & Nakornsri, 1997, Ueno et al., 2012). Permian radiolarians were reported by Saesaengseerung, 2009, Sashida & Nakornsri, 1997 in the Sukhothai, Nakon Sawan, and Uthai Thani provinces, whereas Fusulina and other microfossils were categorized by Fontaine et al., 1996, Ueno et al., 2012 in the Nakon Sawan and Uthai Thani provinces, which are believed to have originated from carbonate rock of the Lampang Group situated within the Sukhothai Zone and of the Saraburi Group corresponded to Indochina Block. Additionally, chronological data, lithological features, and chemical characteristics were investigated using detrital zircon dating from the Sukhothai Zone, revealing the age and origin of clastic sedimentary rocks associated with the subduction system of the Paleo-Tethys Ocean (Hara et al. 2020). In fact, the Central Plain (e.g., Sukhothai, Kampaeng Phet, Nakorn Sawan, Uthai Thani, etc.) is recognized as a component of the Sukhothai Zone, mostly consisting of felsic-mafic volcanic and pyroclastic rocks dating from the Permian-Triassic period (Barr & Charusiri, 2011, Boonsue, 1986). The distribution of the volcanic material not only exposes a granitoid suite in the area from the Early to Late Triassic, but also provides corroborative evidence of the amalgamation between the Sibumasu block and the Indochina block following the most recent phase of the Sukhothai volcanic arc (Barr & Charusiri, 2011, Cobbing, 2011).

Sawan Khalok area, located in the central region of Sukhothai Province, represents a segment of the Sukhothai Zone, revealing the disruption of the Paleo--Tethys Ocean subduction as a volcanic island arc system. The area is predominantly characterized by dispersed mountains, suggestive of Permian rocks, along with granite intrusion outcrops. The geological sequence was characteristically marked for the Pha Haut Formation of the Ngao Group, comprising bedded chert, fine-grained siliciclastic material, and extensively metamorphosed sedimentary rock (DMR, 2008). The Nakon Sawan–Uthai Thani area features a sequence of Permian chert and siliciclastic rocks, classified as a part of Sab Bon Formation within the Saraburi Group (DMR, 2007). The outcrops are scattered broadly in Nakon Sawan and Uthai Thani cities resembling scattered little mountains, which are surrounded by Quaternary sediments from the Chao Phraya River, associated with volcanic rocks and granites (Barr & Charusiri, 2011, Cobbing, 2011).

Our research areas concentrate on both the Sawan Khalok and the Nakon Sawan–Uthai Thani areas, from which we examined chert sections. Many investigations have reported microfossil age, paleo--environment, and geotectonic history (Fontaine et al., 1996, Saesaengseerung, 2009, Sashida & Nakornsri, 1997, Ueno et al., 2012); however, there is limited information regarding the lithological characteristics and occurrences of cherts which restrict understanding of the origins of the cherts and their relationship with country rocks in the Sukhothai Zone. Some papers validated the geological setting for the region using siliceous or carbonate evidence, indicating that certain deposits are associated with the Sibumasu Block while others are in the edges of the Indochina Block (Sashida et al., 2022, Ueno et al., 2012). Therefore, we examine and describe the chert outcrops, addressing depositional age, rock occurrences, geochemical characteristics, and geotectonic implications.

2. Geological outline

The Sukhothai Zone (Bar & Macdonald, 1991, Sone & Metcalfe, 2008, Uneo & Charoentitirate, 2011), or Sukhothai Volcanic Arc, is notably regarded as a disruption of the Paleo-Tethys Ocean, which subducted beneath the outer margins of the Indochina Block (Ueno & Hisada, 1999), extensively spanning the North-South region of central Thailand, particularly from Lampang and Sukhothai to Nakhon Sawan and Uthai Thani provinces (Barr et al., 2000, Boonsue, 1986) **(Fig. 1)**. This volcanic arc zone was developed as part of island-arc system extending to the south as the Chanthaburi Terrane, eastern Thailand. The region exhibits the appearance of pre-Cretaceous mafic to felsic volcanic rocks, as well as Paleozoic mixed siliciclastic-carbonate rocks and metamorphic rocks, which exist as isolated monadnocks (Sashida & Nakornsri, 1997, Ueno et al., 2012). The Paleozoic-Mesozoic rocks serve as the basement for predominantly younger sediments, including Quaternary sediment that constitute alluvial fan, fluvial, and coastal deposits (Choowong, 2011, DMR, 1999). Our research is mostly focused on chert-bearing fine grained siliciclastic rocks, therefore, mainly studied two areas **(Fig. 2A)**: the main one takes place in the Sawan Khalok of Sukhothai Province, situated in the northern part of Central Thailand, while the second is in the Nakon Sawan–Uthai Thani Provinces, located in the southern part of Central Thailand.

The localities of the Sawan Khalok in Sukhothai Province, as shown in **Fig.2B**, approximately 470 km NNW of Bangkok, exhibit poor exposures of the Paleozoic–Mesozoic rocks in flatland. The geological map of the Sukhothai Province indicates that the chert succession has been identified as the Pha Huat Formation of the Ngao Group which composes of thin chert with phyllite and siliceous shale

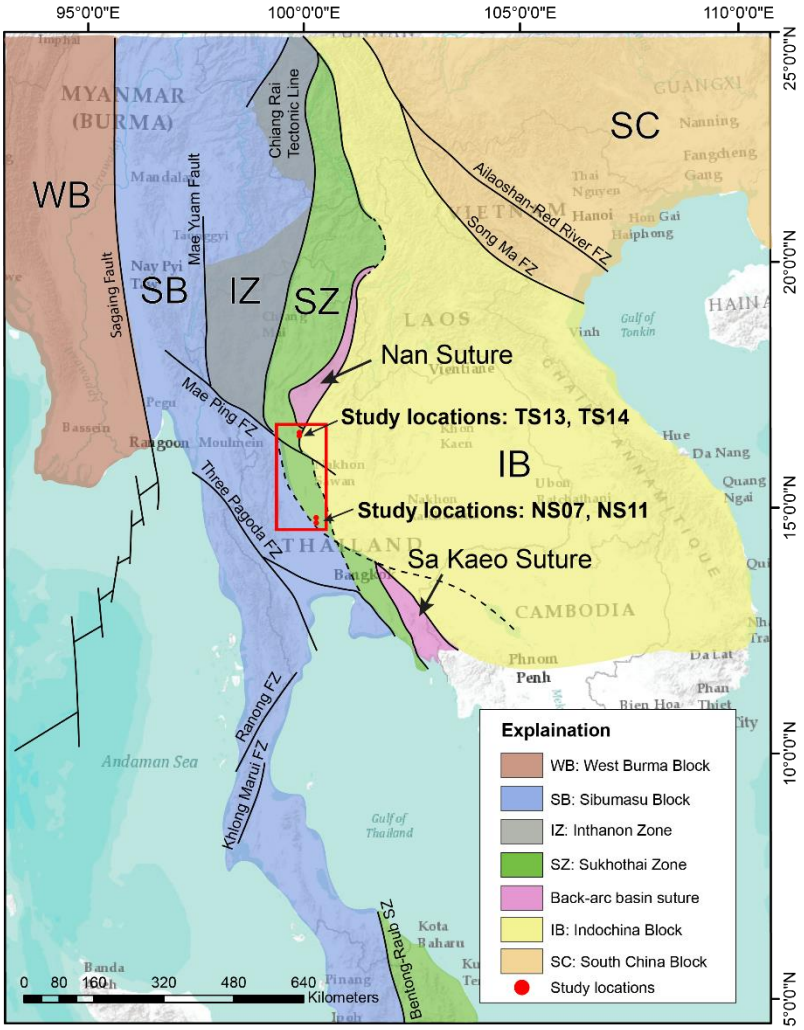

Fig.1: Geotectonic division of Thailand and its surrounding areas (modified after Hara et al., 2020, Metcalfe, 2013, and Ueno et al., 2018), showing four study locations.

interbedded with limestone (DMR, 2008). This region was referred to as Thung Saliam Chert, characterized by noticeable chert formations in several small hills situated between the Sawan Khalok and Thung Saliam, in the northern Sukhothai (Bunopas, 1983), which is re-designed to the Khanu Chert (Bunopas 1974, 1976c) found east of the Khanu Woralaksaburi in Khamphaeng Phet Province. The comprehensive fossil documentation from the Thung Saliam Chert has been accurately dated to the Early Permian age based on radiolarians. *Pseudoalbaillella simplex*, *Ruzencevis-pongus* sp., and *Latentifistulid* gen. et sp. indet. were discriminated from red bedded chert by Sashida & Nakornsri (1997).

Nakon Sawan–Uthai Thani localities, approximately 200 km from Bangkok, include numerous hills oriented in a north-south direction, composed of chert-bearing fine-grained siliciclastic rocks. As DMR, 2007 designated that stratigraphically unit of these rocks in Nakon Sawan city to the Sap Bon Formation of the Saraburi Group **(Fig. 2C)**, described as radiolarian chert, shale interbedded by limestone, and tuff which is controversy with a type section of this formation situated at Ban Sap Bon, Saraburi Province. The original Sap Bon Formation (Hinthong, 1981) is mainly constituted with a succession predominantly of fine-grained siliciclastics such as shale intercalated with siltstone and sandstone, and small outcrops of limestone and chert that it was referred deposition to

Khao Khwang Platform belonging in the Indochina Block. The Khao Gob chert is recognized in the northern region of Nakhon Sawan city **(Fig. 3A)** and plenty of small hills in northern Uthai Thani city (DMR, 1974, 1976). The chert had previously been regarded as Silurian-Devonian in earlier studies (DMR 1999); however, it was subsequently dated to the Early Permian radiolarian age (Saesaengseerung et al. 2007) by fine-grained siliceous rocks in the Nakhon Sawan and Uthai Thani areas, that two distinct radiolarian assemblages are identified: *Pseudoalbaillella lomentaria* Assemblage, indicating an Early Permian (Artinskian), and *Follicucullus scholasticus* Assemblage, corresponding to the late Middle to early Late Permian (Capitanian-Wuchiapingian). Intermediate (diorite and andesite) to felsic (granite, rhyolite and rhyolitic tuff) rocks from the Permian-Triassic were reported in the west Nakhon Sawan (Boonsue, 1986, Jundee et al., 2017). Furthermore, chert-containing fine-grained siliciclastics are present in the northern Uthai Thani city which are also referenced to the Silurian-Devonian Khao Luang tuff (DMR, 2007) because almost the Khao Luang hill is covered primarily of tuffaceous sandstone, phyllitic tuff, and schist. It was believed that forming of the Khao Luang tuff was related with the Triassic granitoid suite (Cobbing, 2011) which huge intruded in the Central Plain of Thailand. Another Permian-Triassic carbonate rocks presumably appear as karsts and monardnocks. Ueno et al. (2012) indicated that Khao Pathawi Triassic limestone is visible in the eastern Uthai Thani Province, which is equivalent to the Triassic Lampang Group, whereas the eastern Nakhon Sawan limestone is classified as part of the Saraburi Group of the Indochina Block.

3. Lithology of Studied sections

Four research sections (NS07, NS11, TS13, and TS14) were examined in the region between Sukhothai and Nakhon Sawan–Uthai Thani Provinces, Thailand **(Fig. 2B & C)**. All these sections are distinguished as stratified cherts. It mostly occurs as scattered monadnocks surrounded by Quaternary sediments, with range strikes oriented about north-south. These small monadnocks are also formed as relatively isolated geomorphic features and exhibit limited continuity with the surrounding country rocks, like granite and volcanic rock. Four stratigraphic sections of radiolaria-bearing bedded chert were measured and samples were systematically collected at one-meter intervals. The lithology, petrography, radiolarian age, and geochemical elements of the chert sequence, Central Plain of Thailand, were examined to elucidate its characteristics and properties.

3.1 Section TS13

A section consisting weakly bedded red chert is obvious as a road cut outcrop on the western hill of Sawan Khalok city, Sukhothai Province (17° 16' 56" N, 99° 42' 25" E). The thickness of the layers range from 5 to 20 cm, with some small quartz vein. An outcrop of silicic shale with quartz veins is also found in the northeast Sawan Khalok **(Fig. 3B)**. This section TS13 is SKT6 of Sashida & Nakornsri (1997). The observation of thin sections **(Fig. 3C)**, a large number of radiolarians together with various microcrystalline quartz veins and the matrix consists of muddy clay are observed in this section.

3.2 Section TS14

This outcrop is in Wat Si Khongkha Ram, Sawan Khalok city, Sukhothai Province (17° 15' 50" N, 99° 41' 59" E), where is far from TS13 approximately 2.5 km south. A thin to thick layer of reddish bedded cherts are clearly exposed at a foothill totally 7 m thickness and other reddish-brown cherts are shown at an upper layer which have similar trending in NNE-SSW directions. Under polarized light microscope, there are abundance of

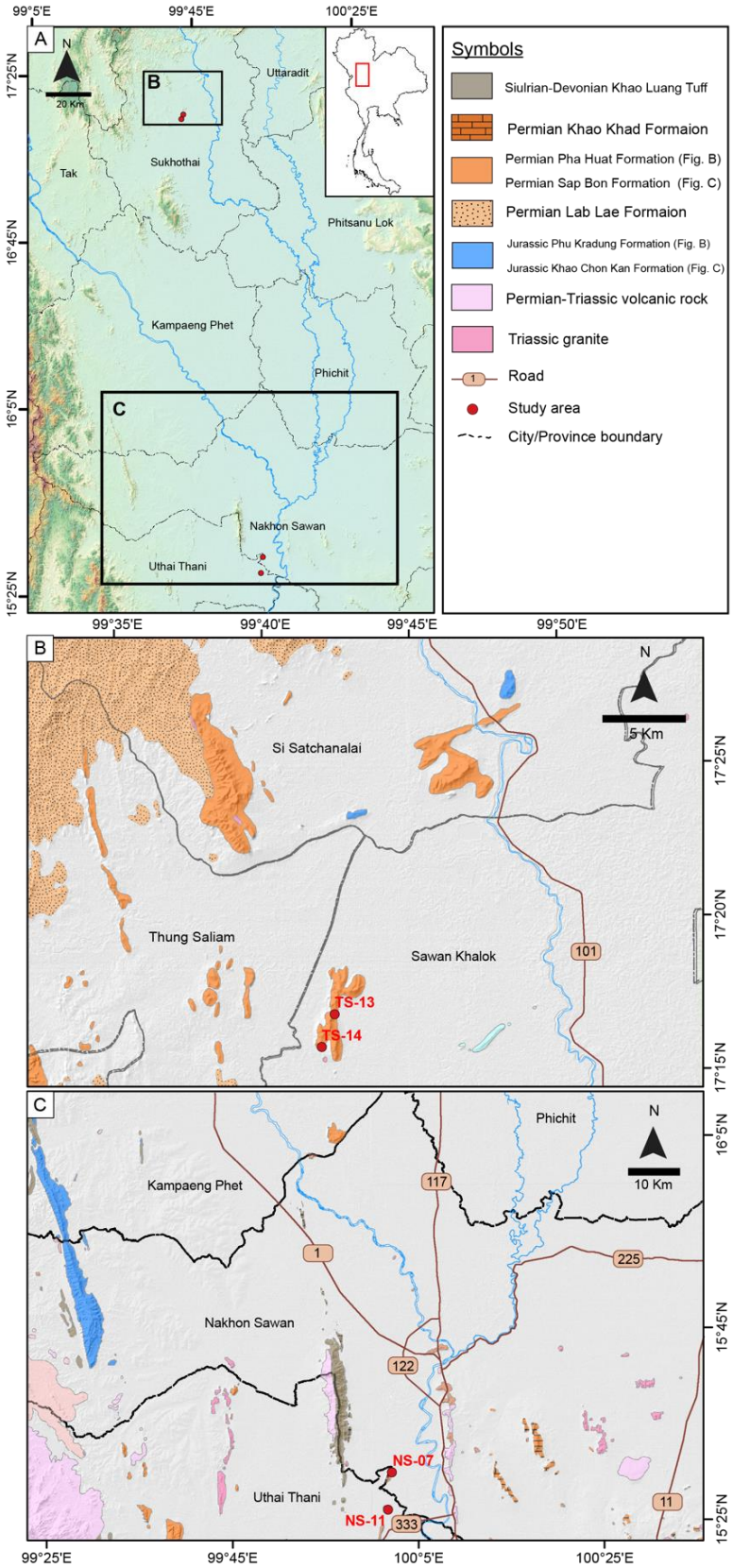

Fig.2: Maps covered the four studied regions in central Thailand. (A) Topographic map outlining the four sampling sites. The red spots mark the locations of the researched sections. (B) Geological map illustrating the two sampling sites in the Sawan Khalok area, modified from DMR (2008), and (C) the two sampling sites in the Nakhon Sawan–Uthai Thani area, modified from DMR (2007).

radiolarian and few sponge spicule traces were filled by microcrystalline quartz with a clay matrix **(Fig. 3D)**. Small quartz veins are not common in the rock texture, but a pressure solution cleavage of muddy clay is clearly observed.

3.3 Section NS07

This study section is located north of Ban Noen Chaeng, Uthai Thani (15° 30' 24" N, 100° 01' 50" E), which is more near Nakon Sawan city than Uthai Thani city approximately 25 km south of Nakon Sawan city **(Fig. 3G)**. The NS07 section consists of a 46 m thick continuous sequence of grey cherts with beds that are 1.5 to several centimeters in thickness. The chert generally shows microcrystalline to cryptocrystalline quartz and matrix of clay **(Fig. 3E)**. Microscopic photo reveals a lot of micro-quartz vein and spherical radiolarian filled with microcrystalline quartz.

3.4 Section NS11

At Ban Nong Phai Baen, Uthai Thani (15° 26' 32" N, 100° 01' 23" E), the road cut outcrop of section NS11 exposes the south of section NS07, approximately 4 km away. The Permian limestone succession of the Saraburi Group surrounds this road cut outcrop, which appears as a single hill in east Uthai Thani Province. A thin layer of gray chert, about 1 to 5 centimeters thickness, is observed, trending in a NNE-SSW direction **(Fig. 3F)**. The thin section observation reveals major compositions of the chert sample compose of microcrystalline to cryptocrystalline quartz, with a clay matrix displaying a pressure solution cleavage. There are also numerous micro-quartz veins, and the radiolarian tests are filled with micro--crystalline quartz.

4. Radiolarians from the Studied Sections and Their Geological Ages

As shown in **Fig. 4**, a total of 27 chert samples were collected from four sections. These samples were treated with hydrofluoric acid (HF) in concentrations ranging from 5% to 10% for approximately 24 hours at room temperature. The extraction procedure was repeated three times to ensure the recovery of sufficient radiolarian specimens suitable for age determination. Residual materials were carefully examined and picked under a stereomicroscope. Radiolarians were successfully extracted from 17 samples. All specimens are archived at the Laboratory of Paleogeosphere Sciences, Department of Geosciences, University of Tsukuba, Japan. Radiolarian age determinations were made based on biostratigraphic studies such as Aitchison et al. (2017a), Ishiga (1986, 1990), Ito & Suzuki (2020), Kuwahara (1999), Kuwahara et al. (1998), and Xiao et al. (2018). Selected, moderately preserved radiolarian specimens are shown in Plate 1.

4.1 Section TS13

Only two samples from this section yielded radiolarians: *Pseudoalbaillella* cf. *annulata* Ishiga, 1984, *Ruzencevispongus* sp., and *Follicucullus* sp. *Pseudoalbaillella annulata* was first reported by Ishiga (1984) and is a diagnostic species of the *Curvalbaillella u-forma* Zone (UAZ 1 of Xiao et al., 2020, 2021), which corresponds to the latest Carboniferous (Gzhelian) to earliest Permian (early Asselian) (Ito & Suzuki, 2022). As previously noted, this section corresponds to SKT6 of Sashida & Nakornsri (1997), where *Pseudoalbaillella simplex* Ishiga & Imoto, 1980, *Ruzencevispongus* sp., and *Latentifistula* sp. have been reported. Based on the occurrence of *Pseudoalbaillella* cf. *annulata* and *Pseudoalbaillella simplex*, this section can be assigned to the *Pseudoalbaillella u-forma m I* to *u-forma m II* Zones (Ishiga, 1986), corresponding to the Asselian.

4.2 Section TS14

Seven chert samples from section TS14 yielded radiolarians, as shown in **Fig 4**. Identified taxa include *Albaillella sinuata* Ishiga et al., 1986, *Albaillella* cf. *asymmetrica*

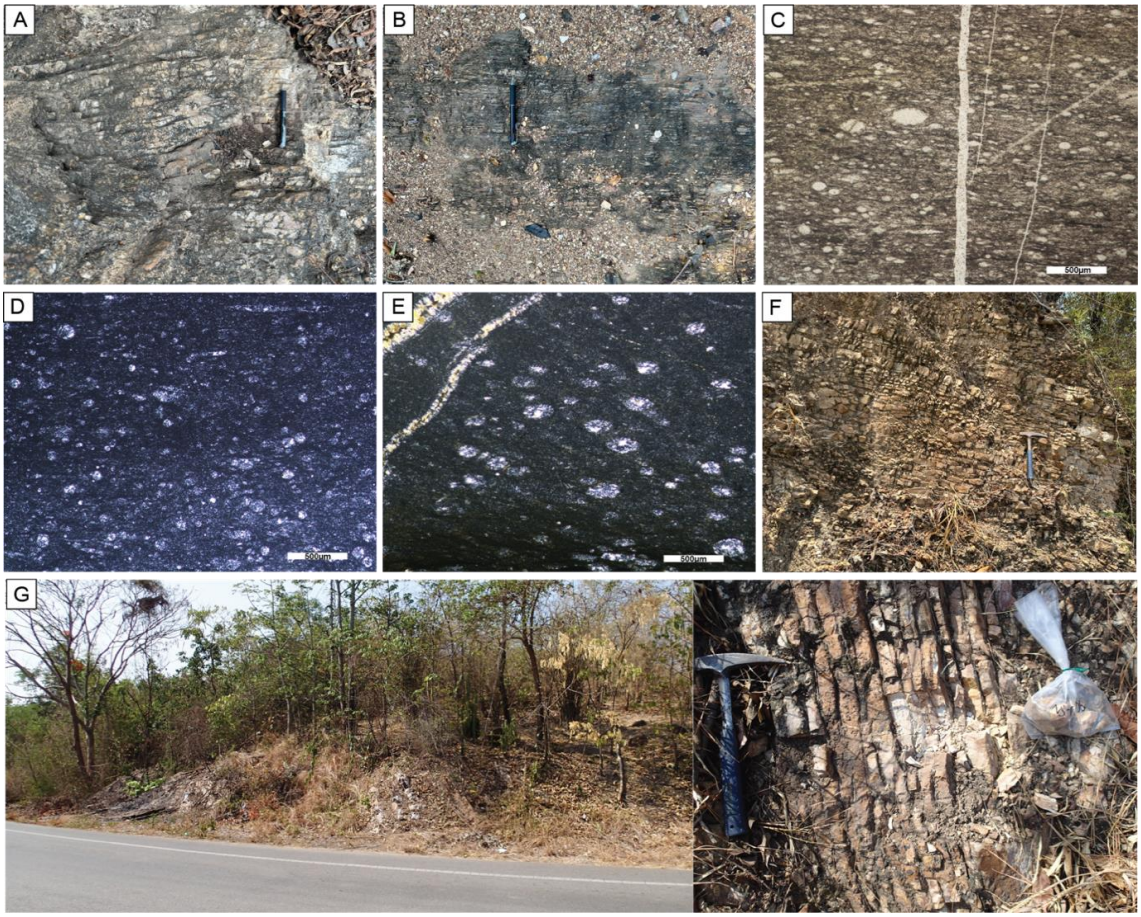

Fig.3: Photographs of outcrops and photomicrographs of chert and siliciclastic rocks. (A) Chert-containing fine-grained siliciclastic rocks found in Nakhon Sawan city (Khao Gob chert). (B) Silicic shale featuring minor and small quartz veins is exposed in the northeastern Sawan Khalok area. (C) Radiolarian-bearing chert from section TS13 seen under plane-polarized light, (D-E) Radiolarian-bearing chert from sections TS14, and NS07 seen under cross-polarized light. (F) Bedded chert (section NS11). (G) Road cut outcrop of NS07 locality showing an outcrop of bedded chert.

Ishiga & Imoto, 1982, *Pseudoalbaillella* cf. *annulata* Ishiga, 1984, *Albaillella* sp., *Pseudoalbaillella* sp., *Follicucullus* sp., and *Ruzencevispongus* sp. *Albaillella sinuata* is known from both the *A. sinuata* and *Parafollicucullus globosus* Zones, corresponding to the late Cisuralian (Kungurian) to early Guadalupian (Roadian) (Xiao et al., 2018). *Albaillella asymmetrica* also occurs within these zones and frequently co-occurs with *A. sinuata*. Although the preservation of the *A.* cf. *asymmetrica* specimen is poor, its co-occurrence with *A. sinuata* suggests that this assemblage likely correlates with the *A. sinuata* and *P. globosus* Zones, thus indicating a late Cisuralian to early Guadalupian age.

4.3 Section NS07

Identified radiolarians from the section NS07 are presented in **Fig. 4**. The radiolarian specimens from these samples exhibit moderate preservation. Identification of species is possible for only five samples: NS07-02, NS07-03, NS07-04, NS07-05 and NS07-07.

Sample NS07-02 contains of *Pseudoalbaillella* cf. *lomentaria* Ishiga & Imoto, 1980, and *Parafollicucullus monacanthus* Ishiga & Imoto, 1980. The presence of *Parafollicucullus monacanthus* suggests an age range from Wordian to Capitanian, corresponding to the *P. monacanthus* to *Follicucullus ventricosus* Zones (Ito & Suzuki, 2022, Xiao et al., 2018).

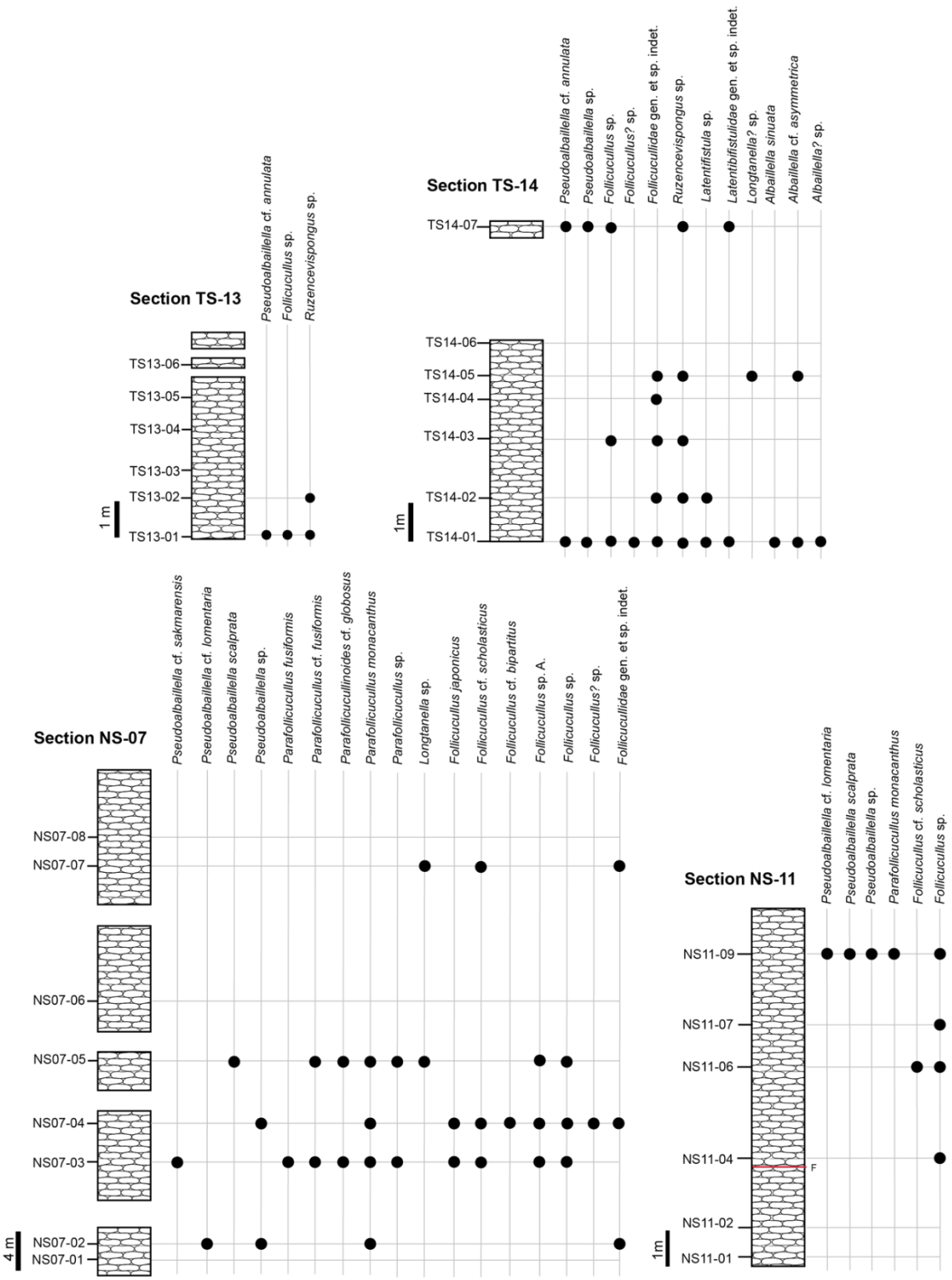

Fig.4: Lithostratigraphic columns and radiolarian occurrence columns in sections of TS13, TS14, NS07, and NS11.

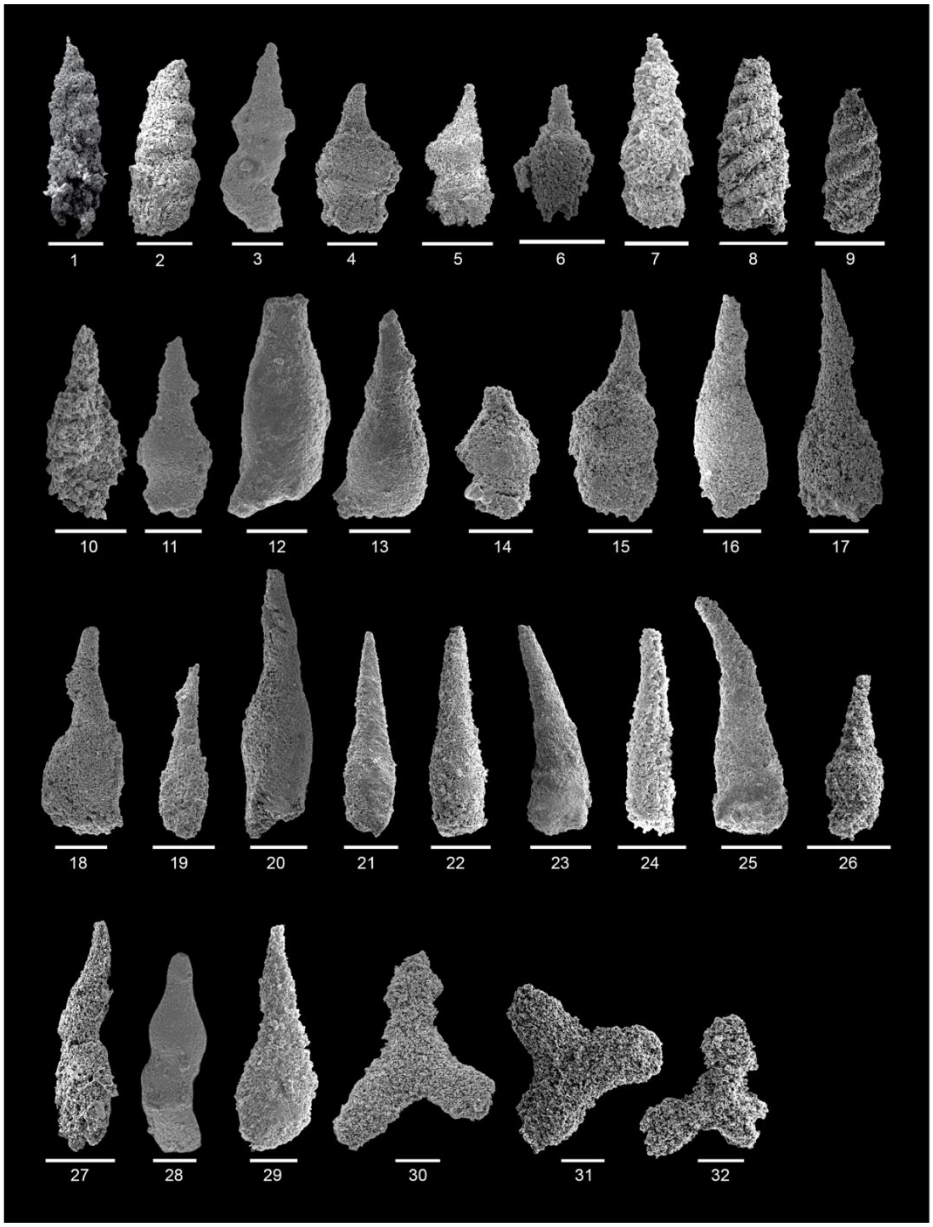

Plate 1: Scanning electron micrographs of radiolarians from cherts of the studied sections TS13, TS14, NS07 and NS11. All scale bars indicate 100 μm. **1.** *Pseudoalbaillella* cf. *annulata* Ishiga, 1984, 004, from TS13-01, **2.** *Pseudoalbaillella* cf. *annulata* Ishiga, 1984, 010, from TS14-01, **3.** *Pseudoalbaillella* cf. *sakmarensis* Kozur, 1981, 24, from NS07-03, **4.** *Pseudoalbaillella scalprata* Holdsworth & Jones, 1980, 07, from NS07-05, **5.** *Pseudoalbaillella scalprata* Holdsworth & Jones, 1980, 013, from NS11-09, **6.** *Pseudoalbaillella scalprata* Holdsworth & Jones, 1980, 019, from NS11-09, **7.** *Pseudoalbaillella* cf. *lomentaria* Ishiga & Imoto, 1980, 001, from NS11-09, **8.** *Albaillella sinuata* Ishiga et al., 1986, 17, from TS14-01, **9.** *Albaillella sinuata* Ishiga et al., 1986, 23, from TS14-01, **10.** *Albaillella* cf. *asymmetrica* Ishiga & Imoto, 1982, 01, from TS14-05, **11.** *Parafollicucullus fusiformis* Holdsworth & Jones, 1980, 29, from NS07-03, **12.** *Parafollicucullus* cf. *fusiformis* Holdsworth & Jones, 1980, 13, from NS07-03, **13.** *Parafollicucullus* cf. *fusiformis* Holdsworth & Jones, 1980, 23, from NS07-05, **14.** *Parafollicucullinoides* cf. *globosus* Ishiga et al., 1982, 04, from NS07-05, **15.** *Parafollicucullinoides* cf. *globosus* Ishiga et al., 1982, 26, from NS07-05, **16.** *Parafollicucullus monacanthus* Ishiga & Imoto, 1980, 13 from NS07-03(2) **17.** *Parafollicucullus monacanthus* Ishiga & Imoto, 1980, 18 from NS07-05 **18.** *Parafollicucullus monacanthus* Ishiga & Imoto, 1980, 36**,** from NS07-05, **19.** *Parafollicucullus monacanthus* Ishiga & Imoto, 1980, 016**,** from NS11-09, **20.** *Follicucullus japonicus* Ishiga, 1991, 20**,** from NS07-03(2), **21.** *Follicucullus* cf. *scholasticus* Rudenko in Belyansky et al., 1984, 10, from NS07-04, **22.** *Follicucullus* cf. *scholasticus* Rudenko in Belyansky et al., 1984, 15, from NS07-04, **23.** *Follicucullus* cf. *scholasticus* Rudenko in Belyansky et al., 1984, 01, from NS07-04(2), **24.** *Follicucullus* cf. *scholasticus* Rudenko in Belyansky et al., 1984, 002, from NS11-06, **25.** *Follicucullus* cf. *bipartitus* Caridroit & De Wever, 1984, 40, from NS07-04, **26.** *Pseudoalbaillella* sp., 08(2), from TS14-07, **27.** *Pseudoalbaillella* sp., 05, from NS07-04(2), **28.** *Follicucullus* sp., 28, from NS07-03, **29.** *Follicucullus* sp., 009, from NS11-09. **30.** *Ruzencevispongus* sp., 015, from TS14-01, **31.** *Ruzencevispongus* sp., 01, from TS14-07, **32.** *Latentifistula* sp., 01, from TS14-02

The age of samples NS07-03 is indicated to range from late Roadian to Capitanian, based on co-occurrence of *Pseudoalbaillella* cf. *sakmarensis* Kozur, 1981, *Parafollicucullus fusiformis* Holdsworth & Jones, 1980, *Parafollicucullinoides* cf. *globosus* Ishiga et al., 1982, *Parafollicucullus monacanthus* and *Follicucullus* cf. *scholasticus* Rudenko *in* Belyansky et al., 1984, which were mainly reported from the *Parafollicucullinoides globosus* to *Follicucullus ventricosus* Zones (Ito and Suzuki, 2022). Other species that are recognized between the Guadalupian period include *Follicucullus japonicus* Ishiga, 1991, and *Follicucullus* A. sp.

Co-occurrence of *Parafollicucullus monacanthus* and *Follicucullus scholasticus* are notable characteristics of Sample NS07-04. According to recent biostratigraphic studies (Ito and Suzuki, 2022, Xiao et al., 2018), this co-occurrence interval of *Parafollicucullus monacanthus* and *Follicucullus* cf. *scholasticus* is limited to the *Follicucullus schlasticus* Zone to *Follicucullus ventricosus* Zone (UAZ 10-11), indicating a middle Capitanian age.

Sample NS07-05 contained radiolarians of *Pseudoalbaillella scalprata* Holdsworth & Jones, 1980, which typically has a range from Sakmarian to Guadalupian. This sample also contains radiolarian specimens identified as *Parafollicucullus* cf. *fusiformis* and *Parafollicucullinoides* cf. *globosus*. *Parafollicucullus fusiformis* is a typical species found in the *Parafollicucullus monacanthus* Zone, and it is known to exist from the Roadian to the late Capitanian time periods. On the other hand, *Parafollicucullinoides globosus* is a key species of the *Parafollicucullus globosus* Zone, and it is believed to have existed from the Roadian to the middle Capitanian. Our specimens were not well preserved and were identified as *Parafollicucullus* cf. *fusiformis* and *Parafollicucullinoides* cf. *globosus,* but it is likely that radiolarians from NS07-05 correspond to the period during which they co-occurred from the Roadian to middle Capitanian.

Specimens from sample NS07-07 were poorly preserved, and only *Follicucullus* cf. *scholasticus*, *Longtanella* sp. and *Follicuculidae* gen. et sp. Indet. were yielded. *Follicucullus scholasticus* is a radiolarian that commonly occurs from late Guadalupian to Lopingian, thus it may indicate an interval from late Guadalupian to Lopingian, but the specific age of the sample NS07-07 is unknown.

Considering the radiolarian ages obtained from the five samples of the section NS07, the Roadian to Capitanian age is herein proposed.

4.4 Section NS11

Radiolarians from section NS11 were generally poorly preserved. Only four samples yielded identifiable taxa, three of which contained only *Follicucullus* sp. as shown in **Fig. 4**. Notably, sample NS11-09 contained *Follicucullus* sp., *Pseudoalbaillella* cf. *lomentaria* Ishiga & Imoto, 1980, *P. scalprata*, *Parafollicucullus monacanthus*, and *Pseudoalbaillella* sp. Considering the co-occurrence of these radiolarian species, the depositional age of samples NS11 can be estimated to be Wordian to Capitanian.

5. Geochemical analyses of the chert

Seventeen samples of bedded cherts are collected from four sections of the Central Plain, Thailand for geochemical analyses. This geochemistry provides an important tool for interpretation of their depositional environment and paleogeography (Aitchison & Flood, 1990, Girty et al., 1996, Murray et al., 1990 Yamamoto, 1987). Major oxides, trace elements, and rare earth elements were analyzed at Activation Laboratories (Actlabs), Canada with the Actlabs' innovative lithium metaborate tetraborate robotic fusion for Inductively Coupled Plasma Mass Spectrometry (ICP/MS) and Inductively Coupled Plasma Emission Spectroscopy

(ICP/OES), controlled by detection limits of the Actlabs. The analytical results for the major, trace, and rare earth elements are listed in Tables 1, 2 and 3, respectively.

5.1 Major elements

The concentrations of the major elements are listed in Table 1. All bedded chert samples from sections TS13, TS14, and NS11 have relatively high concentrations of silica (95.09%–98.30%), represented as typical bedded cherts, containing with silica more than 95%. Meanwhile, the bedded cherts from section NS07 have less concentrations of silica than usual cherts (91.38%–95.53%). High silica contents correspond to small amounts of phosphate, as indicated by the trend in all four areas where silica increases while phosphate decreases. Aluminum (Al) and titanium (Ti) are frequently used as indicators of terrigenous intake in saltwater due to their limited solubility and increased immobility during the diagenesis process. In contrast, metalliferous sediments contain elevated concentrations of iron (Fe) and manganese (Mn), which are considered indicators of hydrothermal activity (Aitchison & Flood, 1990, Yamato, 1987). Al concentrations are considerably high in the chert samples of NS07 and NS11, which are 2.20%–3.50%, and 1.31%–2.09%, respectively, compared to the chert samples of TS13 and TS14, which are 0.56%–0.76%, and 0.47%–o.75%, respectively. There are opposite values in Fe concentrations compared with Al concentrations in which the cherts of TS13 and TS14 exhibit greater values (1.88%–1.90%, and 0.82%–1.68%, respectively), the cherts of NS07 have variable values (0.58%–3.55%), and of NS11 show small values (0.24%–0.38%).

As for Al/(Al + Fe + Mn) ratio, it is a proxy for the influence of hydrothermal contribution in marine sediment and it generally decreases as hydrothermal input increases. A representation of the contribution of hydrothermal influence in marine sediments can be provided by the ratio, which ranges from 0.01% (for hydrothermal cherts) to 0.6 (for biogenic cherts). The TS13 and TS14 cherts, which have The Al/(Al + Fe + Mn) ratios between 0.26–0.32 and 0.25–0.45, record a mixed hydrothermal–biogenic origin, possibly linked to their proximity to hydrothermal sources or spreading center. In contrast, NS07 and NS11, which have the ratios 0.54–0.83 and (0.82–0.91), show a clear biogenic dominance**,** pointing to deposition in more distal or background marine settings. The Al–Fe–Mn diagram of Adachi et al. (1986) is used to identify the depositional origin of siliceous rocks. The diagram exhibits TS13 samples plot in the proximal hydrothermal chert field and show a similar origin to TS14, where two samples fall in the biogenic field and three in the hydrothermal field **(Fig. 5)**. NS07 samples mainly indicate a biogenic origin, and most NS11 chert samples also plot close to the biogenic field. The ratio of $Al_2O_3/(Al_2O_3+Fe_2O_3)$ is a geochemical proxy used to assess the relative contributions of terrigenous and hydrothermal sources to marine sediments. This ratio continuously drops from the continental margin (0.5–0.9) and oceanic basin (0.4–0.7) to the mid-oceanic ridge (0.4) (Murray et al., 1990, 1992). Samples of TS13 and TS14 have similarly ratio (0.23–0.29 and 0.22–0.41) which is apparently contrast with NS07 (0.50–0.81) and NS11 (0.80–0.90). Such the $Al_2O_3/(Al_2O_3+Fe_2O_3)$ ratio, those are lied on the mid-oceanic ridge, pelagic, and continental environment. The discrimination diagrams of $Al_2O_3/(Al_2O_3+Fe_2O_3)$ against Fe_2O_3/TiO_2 (Murray, 1994) indicate that the bedded chert from TS13 and TS14 samples formed in a site close to spreading ridge environment **(Fig. 6)**, whereas NS07 sample formed between an abyssal plain and continental margin, and NS11 sample formed in a continental margin.

Table 1 Content of major elements (wt%) in the chosen chert samples.

Sample	TS13-02	TS13-06	TS14-01	TS14-02	TS14-03	TS14-05	TS14-07	NS07-03	NS07-04	NS07-05	NS07-06	NS07-07	NS11-01	NS11-04	NS11-06	NS11-07	NS11-09
lithology	chert	chert	chert	chert	chert	chert	chert	chert	chert	chert	chert	chert	chert	chert	chert	chert	chert
SiO_2	95.42	95.09	96.57	95.63	96.04	96.28	98.68	93.57	91.38	95.53	95.51	92.87	98.03	95.85	96.54	97.25	98.3
Al_2O_3	0.76	0.56	0.75	0.74	0.47	0.52	0.57	2.45	3.5	2.61	2.2	2.68	1.31	1.67	2.09	1.95	1.22
Fe_2O_3	1.88	1.9	1.33	1.36	1.68	1.5	0.82	0.58	3.55	0.97	1.25	1.19	0.33	0.38	0.24	0.3	0.24
MnO	0.015	0.01	0.012	0.01	0.01	0.012	0.011	0.007	0.013	0.01	0.015	0.016	0.009	0.008	0.007	0.007	0.007
MgO	0.06	0.03	0.07	0.02	0.03	0.04	0.04	0.11	0.13	0.17	0.13	0.08	0.07	0.07	0.07	0.06	0.05
CaO	0.01	0.02	0.01	0.01	0.01	0.01	0.01	0.05	0.03	0.03	0.03	0.01	0.01	0.01	0.01	0.01	0.01
Na_2O	0.01	0.01	0.01	0.02	0.01	0.01	0.01	0.02	0.02	0.02	0.03	0.03	0.01	0.01	0.01	0.01	0.01
K_2O	0.18	0.06	0.22	0.08	0.12	0.13	0.18	0.28	0.38	0.42	0.38	0.28	0.32	0.31	0.3	0.21	0.2
TiO_2	0.028	0.030	0.033	0.023	0.025	0.023	0.023	0.069	0.11	0.09	0.044	0.094	0.023	0.050	0.048	0.060	0.027
P_2O_5	0.03	0.05	0.01	0.02	0.02	0.01	0.01	< 0.01	0.05	0.03	0.05	0.03	0.01	0.01	0.01	0.01	0.01
LOI	0.54	0.89	0.5	0.49	0.41	0.27	0.34	0.97	1.7	0.97	0.93	1.14	0.44	0.64	0.84	0.72	0.53
Total	**98.93**	**98.65**	**99.52**	**98.40**	**98.83**	**98.81**	**100.69**	**98.11**	**100.86**	**100.85**	**100.57**	**98.42**	**100.56**	**99.01**	**100.17**	**100.59**	**100.60**
MnO/TiO_2	0.54	0.33	0.36	0.43	0.40	0.52	0.48	0.10	0.12	0.11	0.34	0.17	0.39	0.16	0.15	0.12	0.26
Al/(Al+Fe+Mn)	0.32	0.26	0.4	0.39	0.25	0.29	0.45	0.83	0.54	0.76	0.67	0.72	0.82	0.84	0.91	0.89	0.86
$Al_2O_3/(Al_2O_3+Fe_2O_3)$	0.29	0.23	0.36	0.35	0.22	0.26	0.41	0.81	0.50	0.73	0.64	0.69	0.80	0.81	0.90	0.87	0.84

Table 2 Concentrations of trace elements (ppm) in the chosen chert samples.

Sample	TS13-02	TS13-06	TS14-01	TS14-02	TS14-03	TS14-05	TS14-07	NS07-03	NS07-04	NS07-05	NS07-06	NS07-07	NS11-01	NS11-04	NS11-06	NS11-07	NS11-09
lithology	chert	chert	chert	chert	chert	chert	chert	chert	chert	chert	chert	chert	chert	chert	chert	chert	chert
Sc	2	2	2	2	2	2	1	3	6	4	3	5	1	2	3	3	2
Be	< 1	< 1	< 1	< 1	< 1	< 1	< 1	< 1	< 1	< 1	< 1	< 1	< 1	< 1	< 1	< 1	< 1
V	26	27	17	17	19	16	12	15	19	20	14	16	7	10	7	11	7
Cr	290	190	230	370	220	220	100	140	150	150	140	170	250	210	220	240	210
Co	3	2	3	4	2	2	1	2	5	2	2	3	3	2	2	3	2
Ni	140	100	110	180	110	110	50	60	80	70	60	80	120	100	110	130	90
Cu	< 10	20	< 10	20	< 10	< 10	< 10	< 10	30	< 10	10	20	< 10	< 10	< 10	< 10	< 10
Zn	< 30	< 30	< 30	< 30	< 30	< 30	< 30	< 30	50	< 30	< 30	< 30	< 30	< 30	< 30	< 30	< 30
Ga	2	2	2	2	1	2	2	4	6	4	4	6	2	3	3	3	3
Ge	1	1.1	0.8	0.8	0.5	0.8	0.8	1.2	1.6	1	1.2	1.5	0.9	1.3	1.5	1.4	1.1
As	5	< 5	< 5	< 5	< 5	< 5	< 5	< 5	5	< 5	< 5	< 5	< 5	< 5	< 5	< 5	< 5
Rb	8	3	8	3	5	5	6	11	15	18	17	12	13	13	13	9	8
Sr	7	9	9	6	8	5	11	17	36	10	48	35	4	4	5	11	5
Y	7	5.5	6.1	4.2	6.4	4.6	4.1	4.5	4.6	5.4	6.6	10.4	3.1	4.5	3.8	5.5	2.3
Zr	12	15	15	15	13	12	15	15	26	20	13	29	8	14	21	17	10
Nb	< 0.2	< 0.2	< 0.2	< 0.2	< 0.2	< 0.2	< 0.2	0.8	1.3	1.1	0.6	0.9	< 0.2	< 0.2	< 0.2	< 0.2	< 0.2
Mo	6	5	5	8	5	5	2	3	4	3	3	4	6	5	6	6	5
Ag	< 0.5	< 0.5	< 0.5	< 0.5	< 0.5	< 0.5	< 0.5	< 0.5	< 0.5	< 0.5	< 0.5	< 0.5	< 0.5	< 0.5	< 0.5	< 0.5	< 0.5
In	< 0.1	< 0.1	< 0.1	< 0.1	< 0.1	< 0.1	< 0.1	< 0.1	< 0.1	< 0.1	< 0.1	< 0.1	< 0.1	< 0.1	< 0.1	< 0.1	< 0.1
Sn	< 1	< 1	< 1	< 1	< 1	< 1	< 1	< 1	1	1	< 1	1	< 1	< 1	< 1	< 1	< 1
Sb	0.4	0.4	< 0.2	0.2	< 0.2	< 0.2	< 0.2	< 0.2	0.2	0.2	0.2	0.2	< 0.2	0.2	< 0.2	0.6	< 0.2
Cs	0.2	0.1	0.2	0.1	0.1	0.1	0.2	0.5	0.6	0.7	0.7	0.5	0.5	0.5	0.5	0.4	0.3
Ba	40	22	54	25	40	40	54	52	72	80	93	105	63	61	61	44	47

Table 3 Concentrations (ppm) of rare earth elements (REEs) in the chosen chert samples.

Sample	TS13-02	TS13-06	TS14-01	TS14-02	TS14-03	TS14-05	TS14-07	NS07-03	NS07-04	NS07-05	NS07-06	NS07-07	NS11-01	NS11-04	NS11-06	NS11-07	NS11-09
lithology	chert	chert	chert	chert	chert	chert	chert	chert	chert	chert	chert	chert	chert	chert	chert	chert	chert
La	6.47	7.17	5.53	5.1	5.86	4.02	2.74	4.89	8.87	6.03	7.79	10.7	2.18	2.43	2.38	5.09	2.38
Ce	6.38	7.29	5.82	5.24	4.88	3.7	2.76	10.7	19.2	14.8	15.7	15.9	3.7	5.63	6.77	12.2	5.94
Pr	1.88	1.98	1.53	1.31	1.62	1.05	0.7	1.26	1.95	1.57	2.05	3.11	0.51	0.56	0.65	1.36	0.62
Nd	8.38	7.94	6.35	5.13	6.21	4.06	2.96	5.16	7.3	6.44	8.36	12.7	1.98	1.93	2.58	5.35	2.37
Sm	2.06	1.89	1.59	1.12	1.52	1	0.63	1.2	1.45	1.33	1.79	2.6	0.44	0.48	0.53	1.18	0.52
Eu	0.50	0.42	0.38	0.25	0.35	0.23	0.18	0.21	0.29	0.30	0.37	0.51	0.09	0.10	0.11	0.23	0.09
Gd	2.01	1.72	1.57	1.1	1.53	1.03	0.84	0.99	1.27	1.27	1.63	2.42	0.4	0.54	0.52	0.99	0.58
Tb	0.29	0.24	0.24	0.17	0.26	0.17	0.14	0.15	0.19	0.18	0.25	0.35	0.06	0.1	0.09	0.16	0.09
Dy	1.63	1.36	1.43	0.96	1.44	0.98	0.81	0.92	1.07	1.13	1.41	2.13	0.4	0.68	0.59	1.02	0.43
Ho	0.3	0.25	0.26	0.19	0.28	0.18	0.15	0.17	0.21	0.22	0.26	0.41	0.09	0.15	0.12	0.21	0.09
Er	0.82	0.7	0.68	0.51	0.75	0.53	0.43	0.48	0.64	0.59	0.72	1.18	0.25	0.43	0.38	0.59	0.27
Tm	0.11	0.10	0.10	0.07	0.11	0.08	0.06	0.07	0.09	0.08	0.09	0.16	0.04	0.07	0.06	0.09	0.04
Yb	0.7	0.64	0.61	0.47	0.69	0.49	0.38	0.42	0.62	0.57	0.55	1.02	0.22	0.42	0.39	0.56	0.24
Lu	0.097	0.093	0.09	0.071	0.101	0.073	0.055	0.062	0.092	0.085	0.075	0.152	0.035	0.06	0.058	0.083	0.036
LREE	27.68	28.41	22.77	19.25	21.97	15.09	10.81	24.41	40.33	31.74	37.69	47.94	9.30	11.67	13.54	26.40	12.50
HREE	3.95	3.39	3.41	2.45	3.63	2.50	2.03	2.27	2.92	2.86	3.36	5.40	1.09	1.91	1.68	2.72	1.20
ΣREE	31.63	31.79	26.18	21.70	25.60	17.59	12.83	26.68	43.25	34.59	41.05	53.34	10.39	13.57	15.22	29.11	13.70
Ce/Ce*	0.40	0.42	0.44	0.44	0.34	0.39	0.43	0.94	1.00	1.05	0.86	0.60	0.76	1.05	1.18	1.01	1.06
Eu/Eu*	1.07	1.01	1.06	1.00	1.00	0.98	1.04	0.84	0.95	1.00	0.96	0.89	0.96	0.83	0.91	0.93	0.70
La_n/Ce_n	2.31	2.24	2.17	2.22	2.74	2.48	2.26	1.04	1.05	0.93	1.13	1.54	1.34	0.98	0.80	0.95	0.91

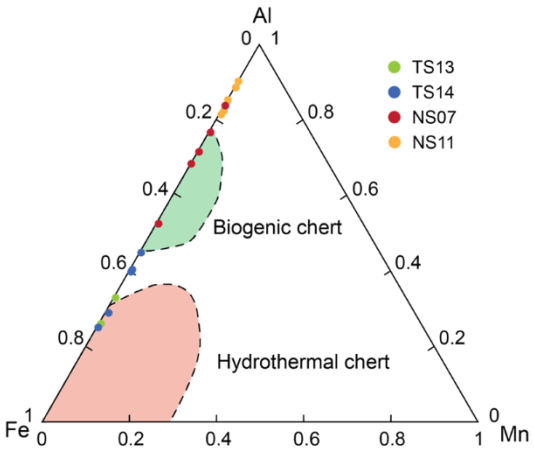

Fig. 5: Triangle diagram of the Al–Fe–Mn elements for the seventeen samples. The biogenic and hydrothermal chert fields originate from Adachi et al. (1986).

5.2 Trace elements

Trace elements are elements mostly present in very small quantities (Table 2), as typically less than 0.1%. Significant concentrations of Cr display outweight other elements that range from 100 – 370 ppm, that there are samples of TS13 and TS14 reach to 300 ppm and samples of NS07 and NS11 fit average in 166 and 226 ppm, respectively. Data for Ni and Cu concentrations appear relatively clustered in chert from continental margin: NS07 has Ni concentrations for 60–80 ppm, NS11 limits for 90–120 ppm., TS13 ranges for 110–140 ppm, and TS14 appears for 50–180 ppm. In addition, the concentrations of Zr and Cr are traditionally associated with detrital heavy minerals, such as zircon, and are potentially more abundant in continental margin chert, which can reflect the source rock of the terrigenous contribution. It shows in the bedded chert of NS07 at 13–29 ppm and NS11 at 8–21 ppm, however not in the cherts of TS13 and TS14 (12–15 ppm and 12–15 ppm, respectively).

Ba concentrations may indicate deposition in upwelling zones or continental margin settings, where productivity is high. In this study, Ba concentrations are also slightly high in samples of NS07 (52–105 ppm), and NS11 (44–63 ppm) compared to samples of TS13 and TS14, which are 22–40 ppm, and 25–54 ppm, respectively. It contains an interestingly high Sr concentration from NS07 sample exceeding 10 ppm (10-48 ppm), that in some cases, hydrothermal fluids can influence Sr concentrations in chert. Elevated Sr levels in chert may indicate proximity to hydrothermal vents or other hydrothermal activity (Andersen and Hume, 1968). Other trace elements in the four areas are low and variable, that some elements are less than 1 ppm and up to a few ppm.

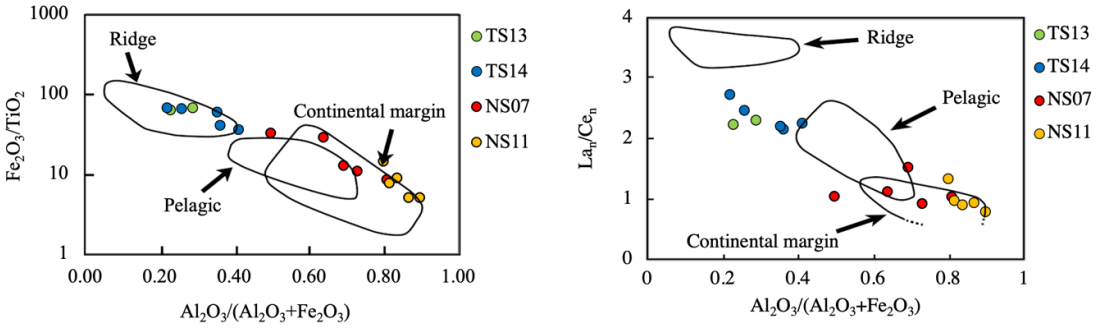

Fig. 6: Diagrams illustrating $Al_2O_3/(Al_2O_3+Fe_2O_3)$ against Fe_2O_3/TiO_2 and La_n/Ce_n effectively distinguish the depositional environments of the Permian bedded cherts within the fields of ridge, pelagic, and continental margin (Murray, 1994).

5.3 Rare earth elements (REEs)

Every REEs contents of the four localities are relatively low, as seen in Table 3, which is less than 1 ppm. A relatively low REEs were obtained from Light Rare Earth Elements (LREEs) and Heavy Rare Earth Elements (HREEs), samples of TS13, TS14, and NS11 also present the relatively low value of the total REEs (ΣREEs) from 31.63 to 31.79, 12.83 to 26.18, and 10.39 to 29.11 ppm, respectively excluded sample of NS07 an intermediate high value of ΣREEs (26.68–53.34). The NASC-normalized La_n/Ce_n and Ce/Ce* ratios are extremely important markers for determinations of tectonic settings and depositional environments presented in marine sediments. Sedimentary settings are evaluated using the La_n/Ce_n ratio, whereas the Ce/Ce* ratio may be found in a wide variety of rocks, ranging from oceanic basins to continental siliceous rocks. Cherts that are deposited along continental margins frequently feature La_n/Ce_n ratios that are close to 1, but those that are deposited on spreading ridges or pelagic settings have greater values, reaching 3.5 and ranging between 2 and 3 (Murray, 1994, Murray et al., 1990). The samples of TS13 and TS14 have a slightly high La_n/Ce_n ratios: TS13 has values between 2.24 and 2.31, and TS14 ranges between 2.17 and 2.74, whilst samples of NS07 and NS11 are a slightly low ranges that La_n/Ce_n ratios: NS07 present values from 0.93 to 1.54, and NS11 appear values from 0.80 to 1.38. Thus, these ratios are lied between the fields of pelagic and continental setting.

In terms of Ce/Ce* ratios, proximal to spreading ridges, average Ce/Ce* values are 0.29, whereas values in the abyssal plain of oceanic basins are 0.6, and continental margins exhibit values of 0.9 (Murray et al., 1990, 1991). The chert samples from TS13 exhibited consistent values Ce/Ce* ratios ranging from 0.40 to 0.42 ppm. The chert samples from TS14 showed slightly low Ce/Ce* ratios, ranging from 0.34 to 0.44 ppm. In contrast, the cherts from N07 and NS11 displayed greater values in 0.60 to 1.05, and 0.76 to 1.18 ppm, respectively. The Ce/Ce* ratios from the four sections suggest a nearby spreading ridge to abyssal plain and terrigenous sediment contributions.

Discrimination diagrams, more particularly $Al_2O_3/(Al_2O_3 + Fe_2O_3)$ vs. La_n/Ce_n (Murray, 1994), provide additional evidence that the chert successions of TS13 and TS14 were deposited in a transitional environment. This environment was located between a mid-oceanic ridge and an oceanic basin. As presented in **Fig. 6**, the NS11 sample was deposited in a continental margin, and the NS07 sample was deposited during transitions from a pelagic plain to a continental zone. Moreover, the chondrite--normalized rare earth element distribution patterns were utilized as labels for the environmental setting of marine sediments. This is because the concentrations of cerium decrease with increasing distance from land. In general, REE patterns of sediments exhibit a strong negative Ce anomaly on a nearby spreading ridge, a negative Ce anomaly in the deep sea, and a positive anomaly on continental margins (Murray et al., 1990, 1991). The chondrite--normalized rare earth element patterns of the analyzed samples from the four sections are illustrated in **Fig. 7**. All profiles exhibit a downward slope, indicating an enrichment of LREEs and a depletion of HREEs. The TS13 section (Asselian) exhibits declared negative Ce anomalies, alike to those in the TS14 section (Kungurian–Roadian). The younger NS07 section (Roadian–Capitanian) exhibits totally no Ce anomalies (flat lines), with only one sample showing a significant negative anomaly. It is similar REE patterns in the NS11 section (Wordian--Capitanian) showing depletions of Ce anomalies.

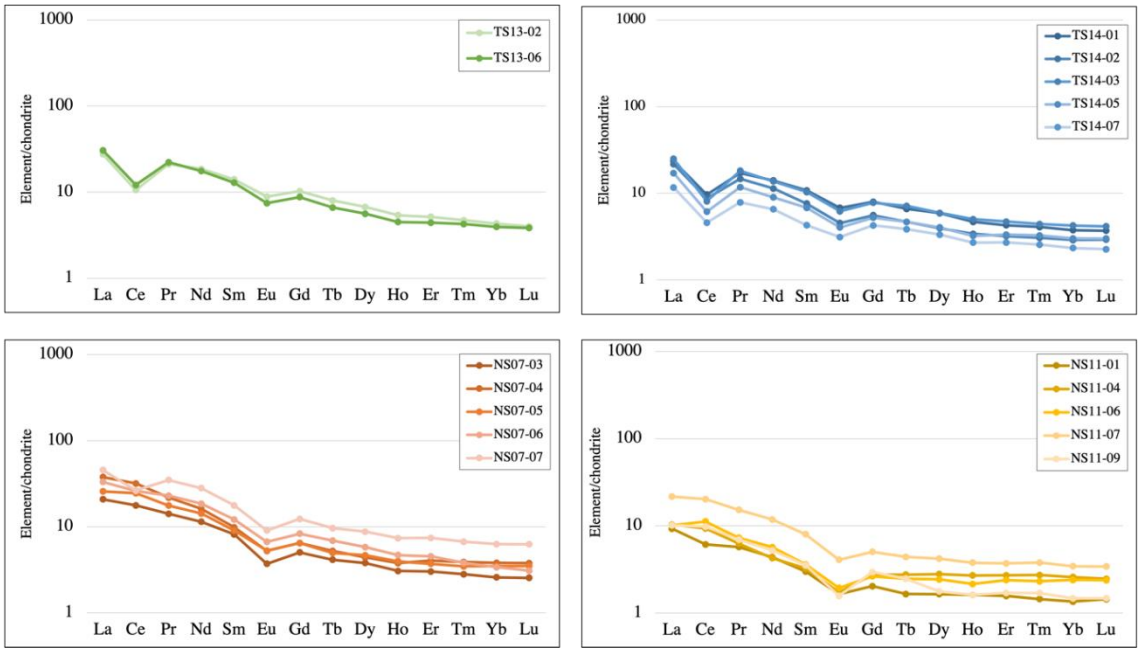

Fig. 7: The distribution patterns of rare earth elements (REE) in the analyzed samples are normalized to chondrite values, as referenced from McDonough & Sun (1995)

6. Discussions

6.1 Relationship of chert successions of the Sawan Khalok area and Nakhon Sawan–Uthai Thani area

The four sections examined in this study are TS13 and TS14 in the Sawan Khalok area, and NS07 and NS11 in the Nakhon Sawan–Uthai Thani area **(Fig. 2)**. The chert exposed in the Sawan Khalok area was named the Khanu Chert by Bunopas (1976, 1981) and assigned to the member of Thung Salium Group (Bunopas, 1981). Whereas the chert in the Nakhon Sawan–Uthai Thani area was described as the Kho Gob Chert (Bunopas, 1976, 1980), and its succession was geologically compared with the Khanu Chert of the Sawan Khalok area (Bunopas, 1981). The geological ages of both the Khanu and Kho Gob Cherts were originally estimated to be Silurian–Devonian by Bunopas (1976, 1981) and Bunopas and Vella (1978). However, the depositional ages of the cherts in both areas were later revised to the Permian based on the occurrence of Permian radiolarians, as reported by Sashida and Nakornsri (1997) and Saesaengseerung et al. (2007). In agreement with these findings, our analysis also yielded Permian radiolarians, confirming that the chert sequences in both areas are of Permian age.

In both areas, the chert successions consist of thin-bedded, reddish to gray or dark gray radiolarian chert. These cherts are interbedded with fine-grained silici-clastic rocks, particularly silicic shale. The successions are consistently oriented in a NNE–SSW direction and typically form small monadnocks. Microscopically, the chert comprises a microcrystalline quartz matrix with clay minerals and an abundance of densely packed radiolarian tests **(Figs. 3C, 3D, 3E)**, while coarse terrigenous grains, such as quartz larger than silt-sized, are absent from the chert layers. These micro-scopic features are typical of pelagic radiolarian bedded chert, which is interpreted to have been deposited in a deep pelagic oceanic setting. This observation also supports the geological correlation of the bedded cherts from both areas (i.e., the Khanu Chert and the Khao Gob Chert).

In summary, the Khanu Chert and the Khao Gob Chert, distributed across the Central Plain of Thailand, are litholo-gically characterized by Permian bedded

radiolarian chert interbedded with siliciclastic rocks such as shale, siltstone, and sandstone. These features are lithologically and stratigraphically comparable to each other, particularly in terms of associated lithologies, microscopic characteristics, and geological ages as determined by radiolarian biostratigraphy. Based on lithological characteristics (thin-bedded radiolarian chert with silicic shale and/or tuffaceous rocks), stratigraphic relationships (consistent interbedding and NNE–SSW orientation), and radiolarian-based age data (Early to Middle Permian), the chert successions in the Sawan Khalok and Nakhon Sawan–Uthai Thani areas are thought to have the same origin.

6.2 Geological comparison with the Permian chert distributed in the Sa Kaeo area, southeastern Thailand

An age determination from radiolarian-bearing cherts in the four locations assigns the age of each section as follows: TS13 (Asselian), TS14 (Kungurian–Roadian), NS07 (Roadian–Capitanian) and NS11 (Wordian–Capitanian), based on radiolarian biostratigraphy. These ages are within the Permian period, similar to chert deposits in the Sa Kaeo suture zone, rather than the extended range of pelagic chert from the Paleo-Tethys Ocean, which spans from the Devonian to Triassic. As discussed in Section 6.1, the lithology and stratigraphy of the studied successions suggest that the Khanu Chert and the Khao Gob Chert could be correlated each other and have the same origin. However, to further evaluate their tectonic origin, a geochemical comparison with other Permian cherts requires more details.

Geochemical analysis of seventeen chert samples across the four sections provides key evidence of depositional settings. The discrimination diagrams, particularly $Al_2O_3/(Al_2O_3 + Fe_2O_3)$ vs Fe_2O_3/TiO_2 and $Al_2O_3/(Al_2O_3 + Fe_2O_3)$ vs La_n/Ce_n (Murray, 1992, 1994), reveal a progression in depositional environments from areas affected by hydrothermal activity to areas affected by terrestrial materials. TS13 on the diagram exhibit low $Al_2O_3/(Al_2O_3 + Fe_2O_3)$ ratios and high Fe_2O_3/TiO_2 ratios, plotting within the ridge-proximal fields **(Fig. 6)**. The cherts were formed a site of the hydrothermal activity **(Fig. 5)**. The Ce/Ce* anomaly values are distinctly low (0.40–0.42), and chondrite-normalized REE patterns show a downward slope with strong negative Ce anomalies **(Fig. 7)**. These signatures are characteristic of deposition influenced by hydrothermal input, likely near a spreading center. TS14 samples plot in both a ridge and a transitional zone between ridge and pelagic fields **(Fig. 6)**, with high Fe_2O_3/TiO_2 ratios and Ce/Ce* values ranging from 0.34 to 0.44. Their chert origins were from hydrothermal and non-hydrothermal activities **(Fig. 5)**. The chondrite-normalized REE patterns exhibit significant negative Ce anomalies along a decreasing slope **(Fig. 7)**. Although still showing hydrothermal characteristics, the influence is weaker than in TS13. This suggests deposition from a site of the hydrothermal activity such as the hydrothermal vent, within a more distal ridge environment. In contrast, samples from NS07 display higher $Al_2O_3/(Al_2O_3 + Fe_2O_3)$ and lower Fe_2O_3/TiO_2 ratios, indicating reduced hydrothermal affect. The discrimination diagram of Murray (1994) plots display a transitional zone **(Fig. 6)**, placing these samples in the open marine to continental margin field. Ce/Ce* values range from 0.60–1.05, and REE patterns become smoother with depleted Ce anomalies. NS11 samples exhibit the most biogenic origin, with $Al_2O_3/(Al_2O_3 + Fe_2O_3)$ ratios exceeding 0.80, and Fe_2O_3/TiO_2 consistently below 10. Ce/Ce* values between 0.76–1.18 and flat Ce anomalies in REE patterns **(Fig. 7)** suggest continental margin influence. All NS07 and NS11samples plot within the biogenic field in the Al–Fe–Mn diagram **(Fig. 5)**, implying deposition deep marine basins where affected by terrestrial materials.

The sequential increase in Ce/Ce* values from TS13, TS14, NS07 to NS11 mirrors a depositional change from areas affected by hydrothermal activity to areas affected by terrestrial materials, arranged in stratigraphic order by age. This trend closely resembles the Sa Kaeo chert succession, where Early Permian cherts reflect deposition near hydrothermal activity, as indicated by strong negative Ce anomalies in REE patterns, high Fe_2O_3/TiO_2 ratios, and their origin with hydrothermal source (Phromsuwan et al., 2024). In contrast, Middle Permian cherts in the Sa Kaeo area show progressively diminished hydrothermal influence, with Ce/Ce* values increasing more than the Early Permian cherts, flattened Ce anomalies in REE profiles, and higher $Al_2O_3/(Al_2O_3 + Fe_2O_3)$ ratios indicated to deposition in abyssal plains or distal continental margins dominated by biogenic origin accumulation (Phromsuwan et al., 2024).

By comparison, Chert sequences of the Inthanon Zone, which is thought to have been deposited in a vast paleoocean of the Paleo-Tethys, has a wide age range over a much longer duration (~250 Ma), ranging from the Middle Devonian to the Middle Triassic (Caridroit, 1993, Kamata et al., 2012, Sashida et al., 2000, and Wonganan et al., 2005). The variations in cerium anomalies in the REE profiles with geological age observed in the Sa Kaeo area have not been reported in the chert sequences of the Inthanon Zone.

Based on depositional time intervals and geochemical evidence, the chert sequences distributed in the Central Plain can be geologically correlated with the Permian chert of the Sa Kaeo area, which is interpreted to have originated in a back-arc basin located between the Sukhothai Arc and the Indochina Block, rather than the chert sequence of the Inthanon Zone, which was deposited in the Paleo-Tethys Ocean. This contrast suggests that the studied successions were formed in a back-arc basin rather than within a vast, long-lived pelagic realm of the Paleo--Tethys.

6.3 Geological affiliation (origin) of the Permian chert distributed in the Central Plain and the extension of the suture in the Central Plain

As previously mentioned, the Chao Phraya Central Plain is widely covered by thick Quaternary sediments, and the Paleozoic to Mesozoic basement rocks are poorly exposed, resulting in a lack of research on their stratigraphy, formation age, and origin. Recently, Ueno et al. (2012) examined the lithology and foraminiferal assemblages of limestone distributed in the Nakhon Sawan and Uthai Thani regions of the Central Plain and proposed a potential tectonic division of the area (see **Figs. 2 and 10** in Ueno et al., 2012).

According to their report, the western parts of Uthai Thani and Nakhon Sawan provinces expose Triassic S-type granite, attributed to the Central Belts (Main Range) of Cobbing (2011), Ordovician limestone correlating with the Thung Song Limestone of the Thai Peninsula (Ridd, 2011), Silurian -Devonian sedimentary rocks corresponding to part of the Thong Pha Phum Group, and the Uthai Thani Limestone, which is comparable to the Ratburi Limestone in the Peninsula. The distribution of these basement rocks suggests that this area belongs to the Sibumasu Continental Block. Conversely, the eastern parts of the Uthai Thani and Nakhon Sawan provinces are underlain by the Tak Fa Formation (a unit of the Saraburi Group) and the Phetchabun Volcanic Belt, which are interpreted as basement rocks associated with the eastern margin of the Indochina Continental Block. Between the basement rocks derived from the Sibumasu and Indochina blocks lies the Permian Khao Kob Chert (the subject of this study) as well as the Khao Pathawi Limestone (defined as a Triassic unit by Ueno et al., 2012) and the Permian?-Triassic

Nakhon Sawan Volcanics. Since the Khao Pathawi Limestone correlates with the Triassic Lampang Group in northern Thailand, Ueno et al. (2012) concluded that this area represents the southern extension of the Sukhothai Zone.

In other words, Central Thailand is divided into three tectonic domains from west to east: the Sibumasu Block, the Sukhothai Zone, and the Indochina Block that it is similar to the configuration observed in northern Thailand. The northwestern extension of the Sa Kaeo Suture, which separates the Sukhothai Zone and the Indochina Block, is inferred to lie between the rocks of Indochina Block origin (mainly the Tak Fa Formation) and those of Sukhothai Zone origin (e.g., the Nakhon Sawan Volcanics). This suggests that the suture extends north–south along the eastern side of Nakhon Sawan (see **Figs. 2 and 10** in Ueno et al., 2012). There are no exposures of ultramafic or mafic rocks such as serpentinite or gabbro, which is typical of suture zones, have been reported in the Chao Phraya Plain. In contrast, Permian bedded cherts containing radiolarians are exposed alongside ultramafic and mafic rocks in the Sa Kaeo and Nan suture zones and are therefore considered critical indicators for identifying sutures.

As mentioned above, the Permian bedded chert (Khao Kob Chert) exposed in the Nakhon Sawan and Uthai Thani areas can be geologically correlated with the Permian bedded chert (Khanu Chert) in the Sawan Khalok area based on age, lithology, stratigraphy, and geochemical characteristics. Accordingly, it is inferred that the Sa Kaeo Suture extends northwestward from the Uthai Thani and Nakhon Sawan areas into the Sawan Khalok area, and continues toward the Nan Suture. The monadnocks containing Permian bedded cherts (NS-07 and NS-11) in the Nakhon Sawan–Uthai Thani areas, as examined in this study, are located slightly west of the inferred position of the Sa Kaeo Suture and lie within the region characterized by Sukhothai Zone rocks, including the Permian–Triassic Nakhon Sawan Volcanics and the Triassic Khao Pathawi Limestone (correlative with the Lampang Group). Although there are no outcrops that directly display the stratigraphic relationship between the cherts and surrounding units, this can be interpreted as the result of tectonic thrusting. The bedded cherts, which are considered part of the suture zone, have been thrust onto the structurally higher units of the Sukhothai Zone due to lateral shortening tectonics associated with the closure of the back-arc basin.

7. Conclusions

Several conclusions can be drawn from this study:

1. The radiolarian assemblages and ages from the Sawan Khalok and Nakhon Sawan–Uthai Thani areas of central Thailand predominantly date to the Early Permian and late Middle Permian, consecutively Asselian from TS13, Kungurian–Roadian from TS14, Roadian–Capitanian from NS07, and Wordian–Capitanian from NS11.

2. Geochemical examinations reveal a distinct depositional environment and origin for each age, indicating that the Early Permian chert (TS13 and TS14) originated from a hydrothermal source and were deposited nearby a spreading ridge zone. The contents of Ce anomalies confirm the considerable negative characteristics in the profile of REE chondrite patterns. The Middle Permian cherts (NS07 and NS11) had a biogenic origin, with NS07 deposited in a transitional zone between a pelagic and a continental margin, while NS11 was deposited in a continental margin region.

3. Based on the radiolarian assemblages and ages, geochemical characteristics, and lithological features,

it appears probable that the chert successions from the Sawan Khalok and Nakhon Sawan–Uthai Thani areas, which have similar origins to the Khanu Chert and the Khao Gob Chert, can be correlated with the back-arc basin cherts from the Sa Kaeo suture zone, despite the absence of outcrops of igneous rock basement.

4. This study proposes that the chert successions documented in the Central Plain, Thailand are considered evidence of radiolarian-bedded chert deriving from the back-arc basin. It is likely that cropping took place because of thrusting followed the closure of the back-arc basin.

References

Adachi, M., Yamamoto, K., & Sugisaki, R. (1986). Hydrothermal chert and associated siliceous rocks from the northern Pacific their geological significance as indication of ocean ridge activity. Sedimentary Geology, 47(1-2), 125–148.

Aitchison, J. C., & Flood, P. G. (1990). Geochemical constraints on the depositional setting of Palaeozoic cherts from the New England orogen, NSW, eastern Australia. Marine Geology, 94(1-2), 79–95.

Aitchison, J.C., Suzuki, N., Caridroit, M., Danelian, T., & Noble, P. (2017a). Paleozoic radiolarian biostratiraphy. Geodiversites, 39, 503–531.

Andersen, N. R., & Hume, D. N. (1968). Determination of barium and strontium in sea water. Analytica Chimica Acta, 40, 207–220.

Barr, S.M., & Charusiri, P. (2011). Volcanic rocks. In: Ridd, M.F.,Barber, A.J., Crow, M.J. (Eds.), The Geology of Thailand. The Geological-Society of London, 4151–439.

Barr, S.M., & Macdonald, A.S. (1991) Toward a late Paleozoic–early Mesozoic tectonic model for Thailand. Journal of Thai Geoscience, 1, 11–22.

Barr, S.M., Macdonald, A.S., Dunning, G.R., Ounchanum, P., & Yaowanoiyothin, W. (2000). Petrochemistry, U–Pb (zircon) age, and palaeotectonic setting of the Lampang volcanic belt, northern Thailand. Journal of the Geological Society, London, 157, 553–63.

Boonsue, S. (1986). Petrography and geochemistry of the volcanic rocks in Changwat Uthai Thani and Nakhon Sawan, Central Thailand (Doctoral dissertation, Chulalongkorn University).

Bunopas, S. (1974). Geologic Map of Changwat Phitsanulok (Sheet NE 47-15, Scale1:250,000). Geological Survey Division, Department of Mineral Resources, Bangkok.

Bunopas, S. (1976). Stratigraphic succession in Thailand. A preliminary summary. Journal of Geological Society of Thailand, 2, 37–58.

Bunopas, S. (1976c). Geology and mineral resources of Changwat Phitsanulok, Sheet NE47-15, Scale 1:250,000. Department of Mineral Resources, Report of Investigation 16 (1/2), 1–217. (in Thai with English summary)

Bunopas, S. (1980). Geology and mineral resources of Changwat Nakhon Sawan, Sheet ND47-3, Scale 1:250,000. Department of Mineral Resources, Geological Survey Report 1, 1–75. (in Thai with English summary)

Bunopas, S. (1981). Palaeogeographic History of Western Thailand and Adjacent Parts of Southeast Asia–A Plate-Tectonic Interpretation: [Dissertation]. University of Wellington, New Zealand. Reprinted as Geological Survey Paper No. 5, 810 p. Department of Mineral Resources, Bangkok, Thailand.

Bunopas, S. (1983). Paleozoic succession in Thailand. In Proceedings of the workshop on stratigraphic correlation of Thailand and Malaysia, 1, 29–76. Geological Societies of Thailand and Malaysia Haad Yai, Thailand.

Bunopas, S., & Vella, P. (1978). Late Palaeozoic and Mesozoic Structural Evolution of Northern Thailand: A Plate Tectonic Model. In: Nutalaya, P., ed., Proceedings of the 3rd Regional Conference on Geology and Mineral Resources of Southeast Asia, Bangkok, 133–140.

Caridroit, M. (1993). Permian radiolaria from NW Thailand. In: Thanasuthipitak, T. (Ed.), Proceedings of the International Symposium on Biostratigraphy of Mainland Southeast Asia, Chiang Mai, January 31–February 5, 1993. Facies and Paleontology. 1, 83–96.

Choowong, M. (2011). Quaternary. In: Ridd, M.F., Barber, A.J., Crow, M.J. (Eds.), The Geology of Thailand. Geological Society, London, 335–350.

Cobbing, E.J. (2011). Granitic rocks. In: Ridd, M.F., Barber, A.J., Crow, M.J. (Eds.), The Geology of Thailand. Geological Society, London, 441–457.

DMR (Department of Mineral Resources of Thailand). (1974). Geological Map of Thailand 1:250,000, Changwat Phitsanulok Sheet, Department of Mineral Resources of Thailand, Bangkok.

DMR (Department of Mineral Resources of Thailand). (1976). Geological Map of Thailand 1:250,000, Changwat Nakornsawan Sheet, Department of Mineral Resources of Thailand, Bangkok.

DMR (Department of Mineral Resources of Thailand). (1999). Geological Map of Thailand, Scale 1:1,000,000. Geological Survey Division, Department of Mineral Resources of Thailand, Bangkok.

DMR (Department of Mineral Resources of Thailand). (2007). Geological Map of Changwat Nakhon Sawan, Scale 1:250,000. Geological Survey Division, Department of Mineral Resources of Thailand, Bangkok.

DMR (Department of Mineral Resources of Thailand). (2007). Report for geological and mineral resource management of Changwat Nakhon Sawan. Geological Survey Division, Department of Mineral Resources of Thailand, Bangkok.

DMR (Department of Mineral Resources of Thailand). (2008). Geological Map of Changwat Sukhothai, Scale 1:250,000. Geological Survey Division, Department of Mineral Resources of Thailand, Bangkok.

DMR (Department of Mineral Resources of Thailand). (2008). Report for geological and mineral resource management of Changwat Sukhothai. Geological Survey Division, Department of Mineral Resources of Thailand, Bangkok.

McDonough, W. F., & Sun, S. S. (1995). The composition of the Earth. Chemical geology, 120(3-4), 223–253.

Feng, Q., Malila, K., Wonganan, N., Chonglakmani, C., Helmcke, D., Ingavat-Helmcke, R., & Caridroit, M. (2005). Permian and triassic radiolaria from northwest Thailand: paleogeographical implications. Revue de Micropaléontologie, 48, 237–255.

Feng, Q., Shen, S., Liu, B., Helmcke, D., Qian, X., & Zhang, W. (2002). Permian radiolarians, chert and basalt from the Daxinshan Formation in Lancangjiang belt of southwestern Yunnan, China. Science in China Series D: Earth Sciences, 45, 63–71.

Fontaine, H., Salyapongse, S., Suteethorn, V., Tansuwan, V., & Vachard, D. (1996). Recent biostratigraphic discoveries in Thailand: a preliminary report. CCOP Newsletter, 21 (2), 14–15.

Girty, G. H., Ridge, D. L., Knaack, C., Johnson, D., & Al-Riyami, R. K. (1996). Provenance and depositional setting of Paleozoic chert and argillite, Sierra Nevada, California. Journal of Sedimentary Research, 66(1), 107–118.

Hada, S. (1999). Asian Accretion of Gondwana-land-derived Terranes and their Final Emplacement: IGCP Project 411. Gondwana Research, 2, 559–61.

Hara, H., Ito, T., Tokiwa, T., Kong, S., & Lim, P. (2020). The origin of the Pailin Crystalline Complex in western Cambodia, and back-arc basin development in the Paleo-Tethys Ocean. Gondwana Research, 82, 299–316.

Hara, H., Kurihara, T., Kuroda, J., Adachi, Y., Kurita, H., Wakita, K., ... & Chaodumrong, P. (2010). Geological and geochemical aspects of a Devonian siliceous succession in northern Thailand: implications for the opening of the Paleo-Tethys.Palaeogeography,Palaeoclimato-logy, Palaeoecology, 297(2), 452–464.

Hinthong, C., (1981). Geology and Mineral Resources of Changwat Phra Nakhon Si Ayutthaya (ND 47–8), Scale 1:250,000. Department of Mineral Resources, Geological Survey Report 4, 1–105. (in Thai with English summary)

Holdsworth B. K., & Jones D. L. (1980). Preliminary radiolarian zonation for late Devonian through Permian time. Geology, 8 (6), 281–285.

Ishiga, H. (1984). Follicucullus (Permian Radiolaria) from Maizuru Group in Maizuru Belt, Southwest Japan. Earth Science (Chikyu Kagaku), 38(6), 427–434a.

Ishiga, H. (1986). Late carboniferous and permian radiolarian biostratigraphy of southwest Japan. Journal of Geosciences, Osaka City University, 29, 89–100.

Ishiga, H. (1990). Paleozoic Radiolarians. In Ichikawa K., Mizutani, S., Hara, I., Hada, S. and Yao, A., eds., Pre-cretaceous Terranes of Japan, IGCP Project, no. 224, 285–295.

Ishiga, H. (1991). Description of a new Follicucullus species from Southwest Japan. *Mem. Fac. Sci., Shimane Univ.*, *25*, 107-118.

Ishiga, H., & Imoto, N. (1980). Some Permian radiolarians in the Tamba district, Southwest Japan. Earth Science (Chikyu Kagaku), 34, 333–345.

Ishiga, H., Kito, T., & Imoto, N. (1982). Late Permian radiolarian assemblages in the Tamba district and an adjacent area, Southwest Japan. Earth Science (Chikyu Kagaku), 36, 10–22.

Ishiga, H., Watase, H., & Naka, T. (1986). Permian radiolarians from Nishiki Group in Sangun-

Chugoku Belt, Southwest Japan. Earth Science (Chikyu Kagaku), 40(2), 124–136c.

Ito, T., & Suzuki, N. (2022). Recent progress on research of Permian radiolarian Follicucullidae, Fossils (The Palaeontological Society of Japan), 112, 5–16 (in Japanese).

Ito, T., Hara, H., Kong, S., & Lim, P. (2020). New materials of Cisuralian (early Permian) radiolarians from western Cambodia: Paleobiogeographic implications in the Paleotethys. Palaeoworld, 29, 568–576.

Jundee, P. K., Limtrakun, P., Boonsoong, A., & Panjasawatwong, Y. (2017). Petrography and REE geochemical characteristics of felsic to mafic volcanic/hypabyssal rock in Nakhon Sawan and Uthai Thani Provinces, Central Thailand. *Chiang Mai J Sci*, *4*, 1722–1734.

Kamata, Y., Chutakositkanon, V., Hisada, K., Charusiri, P., & Ueno, K. (2003). Permian radiolarians from the Sa Kaeo–Chanthaburi area, eastern part of Thailand. Proceedings of 1st International Conference on Palaeontology of Southeast Asia, Mahasarakham, 27–30. Mahasarakham University Journal vol. 22 (Special Issue), 249–250.

Kamata, Y., Maezono, A., Hara, H., Ueno, K., Hisada, K., Sardsud, A., Charoentitirat, T., & Charusiri, P. (2012). Basaltic activity preserved in an Upper Permian radiolarian chert from the Paleo-Tethys in the Inthanon Zone, northern Thailand. J. Asian Earth Sci, 61, 51–61.

Kamata, Y., Ueno, K., Hara, H., Charoentitirat, T., & Charusiri, P. (2018). Paleozoic and Mesozoic Back-arc basin chert of the Paleo-Tethys in Thailand, Proceedings of the Second International Symposium on Geoscience Resources and Environments of Asian Terranes (Great 2018) 19–23 November, 2018, Bangkok, Thailand.

Kozur, H. (1981). Albaillellidae (Radiolaria) aus dem Unterperm des Vorurals. *Geologische-Palaaontologische Mitteilungen Innsbruck*, *10*, 263-274.

Kuwahara, K. (1999). Phylogenetic Lineage of Late Permian *Albaillella* (*Albaillellaria*, Radiolaria). Journal of Geosciences, Osaka City University, 42, 85–101.

Kuwahara, K., Yao, A., & Yamakita, S. (1998). Reexamination of Upper Permian radiolarian biostratigraphy. Earth Science – (Chikyu Kagaku). Journal of the Association for the Geological Collaboration in Japan, 52, 391–404.

Metcalfe, I. (2013). Gondwana dispersion and Asian accretion: Tectonic and palaeogeographic evolution of eastern Tethys. Journal of Asian Earth Sciences, 66, 1–33.

Metcalfe, I. (2021). Multiple Tethyan ocean basins and orogenic belts in Asia, Gondwana Research, 100, 87–130.

Murray, R.W. (1994). Chemical criteria to identify the depositional environment of chert: general principles and applications. Sedimentary Geology, 90, 213–232.

Murray, R.W., Buchholtz ten Brink, M.R., Jones, D.L., Gerlach, D.C., & Russ III, G.P. (1990). Rare earth elements as indicators of different marine depositional environments in chert and shale. Geology, 18, 268–271.

Murray, R.W., Ten Brink, M.R.B., Gerlach, D.C., Russ III, G.P., & Jones, D.L. (1991). Rare earth, major, and trace elements in chert from the Franciscan Complex and Monterey Group, California: assessing REE sources to fine-grained marine sediments. Geochimica et Cosmochimica Acta, 55, 1875–1895.

Murray, R.W., Ten Brink, M.R.B., Gerlach, D.C., Russ III, G.P., & Jones, D.L. (1992). Rare earth, major, and trace element composition of Monterey and DSDP chert and associated host sediment: Assessing the influence of chemical fractionation during diagenesis. Geochimica et Cosmochimica Acta, 56, 2657–2671.

Phromsuwan, W., Kamata, Y., Hayashi, T., Kobayashi, K. I., Charoentitirat, T., Ueno, K., & Sardsud, A. (2024). Radiolarian age and geochemical characteristics of the Permian bedded chert sequence in the Soi Dao area, Chanthaburi, Southeast of Thailand. Revue de Micropaléontologie, 85, 100786.

Rudenko (1984), in Belyansky G. S., Nikita A. P., & Rudenko V. S., 1984. About Sebuchaz suite of Primorye, in Poya rkova Z. N. (ed.), New Data an Detail Biostratigraphy of Phanerozoic of Far East. DVNC Akademii Nauk SSSR, Vladivostok, 43-57.

Saesaengseerung, D. (2009). Devonian to Triassic radiolarian biostratigraphy and depositional environments of these radiolarian-bearing rocks in Thailand, 220 p. PhD Thesis, University of Tsukuba, Tsukuba.

Saesaengseerung, D., Agematsu, S., Sashida, K., & Sardsud, A. (2009). Discovery of Lower Permian radiolarian and conodont faunas from the bedded chert of the Chanthaburi area along the Sra Kaeo suture zone, eastern Thailand. Paleontological Research, 13, 119–138.

Saesaengseerung, D., Sashida, K., Sardsud, A., & Poonpan, S. (2007). Discovery of Permian radiolarian faunas from the Nakhon Sawan and

Uthai Thani areas, Central Thailand. In: Tantiwanit, W. (Ed.), Proceedings of the International Conference on Geology of Thailand (GEOTHAI'07): Towards Sustainable Development and Sufficiency Economy. Department of Mineral Resources, Bangkok, 72.

Sashida, K., Adachi, S., Igo, H., Nakornsuri, N., & Ampornmaha, A. (1997). Middle to Upper Permian and Middle Triassic radiolarians from Eastern Thailand, Science Reports of the Institute of Geoscience University of Tsukuba, section B=Geological Sciences, v. 18, 1–17.

Sashida, K. & Nakornsri, N. (1997). Lower Permian radiolarian faunas from the Khanu Chert Formation distributed in the Sukhothai area, northern central Thailand. In, Dfeeradilok, P.et al. eds., Proceedings of the International Conference on Stratigraphy and Tectonic Evolution of Southeast Asia and the South Pacific, Bangkok, 19–24.

Sashida, K., Igo, H., Hisada, K., Ueno, K., Kajiwara, Y., Nakornsri, N., & Sardsud, A. (2000). Late Permian to Middle Triassic radiolarian faunas from northern Thailand. Journal of Paleontology, 74, 789–811.

Sashida, K., Ito, T., Hong, P., Fukushima, Y., Agematsu, S., Salyapongse, S., & Putthapiban, P. (2022). Occurrence of early Carboniferous radiolarians and Middle Triassic conodonts from Ban Rai, southwestern Uthai Thani, central Thailand and its geological significance. Paleontological Research, 26(4), 420–439.

Sone, M., & Metcalfe, I. (2008). Parallel Tethyan sutures in mainland Southeast Asia: New insights for Palaeo-Tethys closure and implications for the Indosinian orogeny. Comptes Rendus Geoscience, 340(2-3), 166–179.

Udchachon, M., Thassanapak, H., & Burrett, C. (2018). Early Permian radiolarians from the extension of the Sa Kaeo Suture in Cambodia–tectonic implications. Geological Magazine, 155, 1449–1464.

Ueno, K., & Charoentitirat, T. (2011). Carboniferous and Permian. In: Ridd, M.F.,Barber, A.J., Crow, M.J. (Eds.), The Geology of Thailand. The Geological Society of London, 71–136.

Ueno, K., & Hisada, K. 1999. Closure of the Paleo-Tethys caused by the collision of Indochina and Sibumasu. Chikyu Monthly, 21, 832–839 (in Japanese).

Ueno, K., Kamata, Y., Uno, K., Charoentitirat, T., Charusiri, P., Vilaykham, K., & Martini, R. (2018). The Sukhothai Zone (Permian–Triassic island-arc domain of Southeast Asia) in Northern Laos: insights from Triassic carbonates and foraminifers. Gondwana Research, 61, 88–99.

Ueno, K., Miyahigashi, A., Kamata, Y., Kato, M., Charoentitirat, T., & Limruk, S. (2012). Geotectonic implications of Permian and Triassic carbonate successions in the Central Plain of Thailand. Journal of Asian Earth Sciences, 61, 33–50.

Wonganan, N., & Caridroit, M. (2005). Middle and Upper Devonian radiolarian faunas from Chiang Dao area, Chiang Mai province, northern Thailand. Micropaleontology, 51, 39–57.

Xiao, Y. F., Suzuki, N., & He, W. H. (2018). Low-latitudinal standard Permian radiolarian biostratigraphy for multiple purposes with Unitary Association, Graphic Correlation, and Bayesian inference methods. Earth-Science Reviews, 179, 168–206.

Xiao, Y., Suzuki, N., He, W., Benton, M. J., Yang, T., & Cai, C. (2020). Verifiability of genus-level classification under quantification and parsimony theories: a case study of follicucullid radiolarians. Paleobiology, 46(3), 337–355.

Xiao, Y., Suzuki, N., Ito, T., & He, W. (2021). New Permian radiolarians from east Asia and the quantitative reconstruction of their evolutionary and ecological significances. Scientific Reports, 11(1), 6831.

Yamamoto, K. (1987). Geochemical characteristics and depositional environments of cherts and associated rocks in the Franciscan and Shimanto Terranes. Sedimentary Geology, 52(1-2), 65–108.